

# Structure Oriented Compact Model for Advanced Trench IGBTs without Fitting Parameters for Extreme Condition: Part II

著者	Takaishi J., Harada S., Tsukuda M., Omura I.
journal or publication title	Microelectronics reliability
volume	54
number	9-10
page range	1891-1896
year	2014-09-05
URL	<a href="http://hdl.handle.net/10228/5767">http://hdl.handle.net/10228/5767</a>

doi: info:doi/10.1016/j.microrel.2014.07.158

# Structure oriented compact model for advanced trench IGBTs without fitting parameters for extreme condition: part II

J. Takaishi<sup>a,\*</sup>, S. Harada<sup>a</sup>, M. Tsukuda<sup>b</sup>, I. Omura<sup>a</sup>

<sup>a</sup> Kyushu Institute of Technology, 1-1 Sensui-cho, Tobata-ku, Kitakyushu, 804-8550, Japan

<sup>b</sup> The International Centre for the Study of East Asian Development, 1-8 Hibikino, Wakamatsu-ku, Kitakyushu, Japan

## Abstract

Compact model for expressing turn-off waveform for advanced trench gate IGBTs is proposed even under high current density condition. The model is analytically formulated only with device structure parameters so that no fitting parameters are required. The validity of the model is confirmed with TCAD simulation for 1.2 kV to 6.5 kV class IGBTs. The proposed turn-off model is sufficiently accurate to calculate trade-off curve between turn-off loss and saturation collector voltage under extremely high current conduction, so that the model can be used for system design with the advanced trench gate IGBTs.

## 1. Introduction:

Advanced IGBTs with the special scalable miniaturization of the structure exhibit feature of extremely high current conduction capability thanks to high stored carrier in the N-Base layer (see Fig. 1) [1-4]. The IGBT scaling principle is similar, however it is different from the general CMOS scaling principle [5]. The principle realizes both shallower cathode structure and higher electron injection efficiency than the conventional structure. It leads higher carrier concentration in the emitter side and lower saturation collector voltage.

Since the commercialization of the IGBT, semiconductor industries have made great technological advancement in improving device performance [6-17]. Especially current density of the

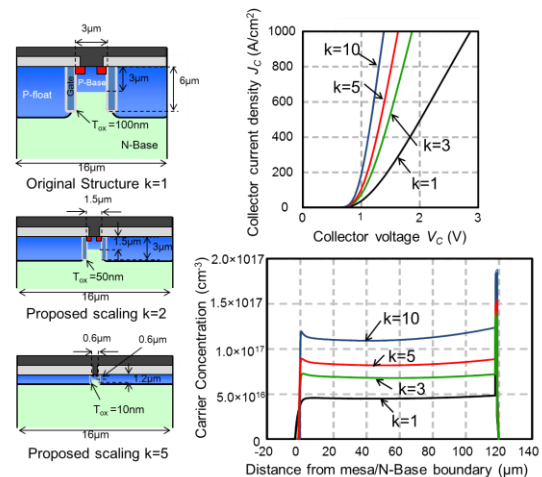


Fig. 1. Advanced trench IGBT with the special miniaturized structure[1-4].

\* Corresponding author. n349514j@mail.kyutech.jp and omura@ele.kyutech.ac.jp  
Tel: +81 (93) 884 3268; Fax: +81 (93) 884 3268

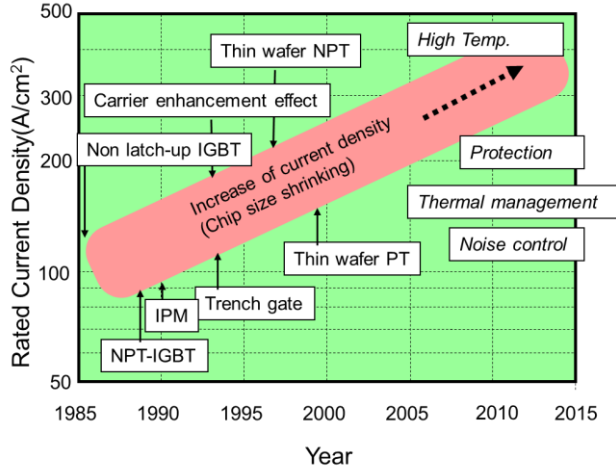


Fig. 2. Evolution of IGBT technology over the last 20 years[6,7].

IGBT has increased for more than 25 years (see Fig. 2). The improvement has been achieved by optimizing device cell pattern, introducing trench gate structures, and optimizing vertical IGBT structure.

We already proposed analytical model for the on-state of the advanced IGBT in previous research [1-3]. The compact model eliminates the fitting parameters in the model equations and only uses the device structure parameters. This concept enables the new model to be used in extreme condition and expands the compact model function from circuit optimization to circuit device coupled optimization since the model can be applicable for wide range of device structure.

In this paper, we propose new formulation for the high current turn-off of the advanced IGBT considering the dynamic avalanche phenomena. In order to predict the trade-off curve between saturation collector voltage and turn-off loss, high current turn-off characteristics are required in addition to the analytical model for the on-state. The dynamic avalanche phenomena can occur during high current turn-off transient so the compact model for the advanced IGBT switching needs to include the dynamic avalanche phenomena in the formulation since the phenomena affects the turn-off losses and dynamic collector voltage waveform [18].

## 2. New formulation of IGBT turn-off

The turn-off waveform is analytically modelled considering dynamic avalanche phenomena during

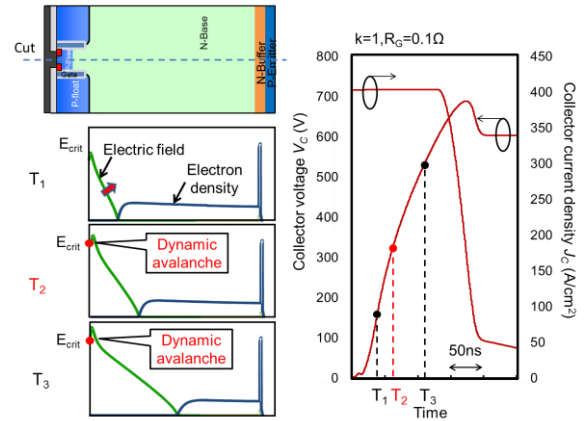


Fig. 3. Relation of carrier distribution and electric field during the high current turn-off. The dynamic avalanche occurred in turn-off transient.

high current turn-off. When the dynamic avalanche starts, generated electrons compensate the electric field in the N-Base so  $dV_C/dt$  is lowered than before dynamic avalanche (see Fig. 3). The detail of proposed model formulations for the high current turn-off of the advanced IGBT is in the subsection 2.1 and 2.2. The turn-off model has been verified by comparing with TCAD simulation in the subsection 2.3.

### 2.1. New formulation before dynamic avalanche

Electric field in the N-Base layer before dynamic avalanche is simply expressed by Poisson equation as below.

$$E(t) = \frac{q}{\epsilon} \left( N_D + \frac{J_{p,D}}{qv_{sp}} \right) W(t) \quad (1)$$

where,  $E$  is electric field,  $q$  is charge of electron,  $\epsilon$  is silicon's permittivity,  $N_D$  is N-Base concentration,  $J_{p,D}$  is hole current density in the depletion layer,  $v_{sp}$  is hole saturation velocity,  $W$  is depletion layer length.

Hole current density  $J_{p,D}$  is equal to total current density ( $J_{p,D}=J_C$ ). Thus

$$E(t) = \frac{q}{\epsilon} \left( N_D + \frac{J_C}{qv_{sp}} \right) W(t) \quad (2)$$

Turn-off collector voltage  $V_C$  is expressed as

$$V_C = \frac{1}{2} E(t)W(t) \quad (3)$$

Substituting Eq. (2) into Eq. (3), yields

$$V_C = \frac{q}{2\epsilon} \left( N_D + \frac{J_C}{qv_{sp}} \right) W^2(t) \quad (4)$$

Collector voltage  $V_C$  waveform can be calculated by Eq. (4). In this equation,  $W$  can be obtained by integration of  $dW/dt$  as below.

Before dynamic avalanche, we assume that no electron current flows in the depletion layer from n-channel. So electron current density in the stored carrier  $J_n$  only affects the expansion of depletion layer (see Fig. 4), so the expansion of the depletion layer is expressed as

$$\frac{dW}{dt} = \frac{J_n}{qn(x)} \quad (5)$$

where,  $W$  is depletion layer length,  $q$  is charge of electron,  $J_n$  is electron current density in the stored carrier,  $n(x)$  is stored carrier concentration of N-Base region. The depletion layer length  $W$  is obtained by integration of Eq. (5) for Eq. (4). In this equation,  $J_n$  can be obtained as below

The electron current density  $J_n$  and hole current density  $J_p$  in the stored carrier is expressed by next elementary formula.

$$J_n = q\mu_n n(x) E_{st} + kT\mu_n \frac{dn}{dx} \quad (6)$$

$$J_p = q\mu_p p(x) E_{st} - kT\mu_p \frac{dp}{dx} \quad (7)$$

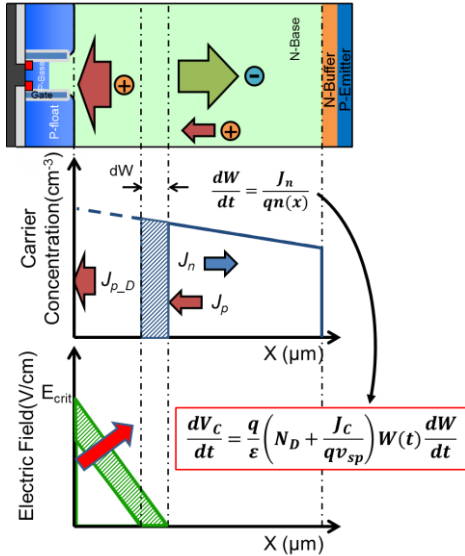


Fig. 4. Turn-off mechanism before dynamic avalanche and the formulation.

where,  $\mu_n$  and  $\mu_p$  are electron and hole mobility,  $E_{st}$  is electric field in the stored carrier,  $k$  is Boltzmann constant,  $T$  is temperature.

In conductive modulation condition,  $n(x) = p(x)$  can be assumed. Adding Eq. (6) and Eq. (7),

$$E_{st} = \frac{J_n + J_p}{q(\mu_n + \mu_p)n(x)} - kT \frac{\mu_n - \mu_p}{\mu_n + \mu_p} \frac{dn}{dx} \quad (8)$$

Total current density  $J_c$  is sum of electron current density  $J_n$  and hole current density  $J_h$  ( $J_c = J_n + J_p$ ). So Eq. (8) is expressed as

$$E_{st} = \frac{J_c}{q(\mu_n + \mu_p)n(x)} - kT \frac{\mu_n - \mu_p}{\mu_n + \mu_p} \frac{dn}{dx} \quad (9)$$

Substituting Eq. (9) into Eq. (6), yields

$$J_n = \frac{\mu_n}{\mu_n + \mu_p} \left( J_c + 2kT\mu_p \frac{dn}{dx} \right) \quad (10)$$

Eq. (10) expresses the electron current density in stored carrier  $J_n$  for Eq. (5). If the differential of initial carrier distribution  $dn/dx$  is constant, the electron current density  $J_n$  is also assumed as constant.

## 2.2. New formulation after dynamic avalanche

Differential of turn-off voltage  $dV_C/dt$  after dynamic avalanche can be expressed as

$$\frac{dV_C}{dt} = \frac{1}{2} E_{crit} \frac{dW}{dt} \quad (11)$$

Collector voltage  $V_C$  waveform can be calculated by integration of Eq. (11). Critical electric field for dynamic avalanche  $E_{crit}$  is almost determined by material.

Differential of depletion layer  $dW/dt$  after the dynamic avalanche can be expressed by electron current densities in the depletion layer and stored carrier (see Fig. 5).

$$\frac{dW}{dt} = \frac{J_n - J_{n,D}}{qn(x)} \quad (12)$$

where,  $J_{n,D}$  is electron current density in depletion layer. In the equation,  $J_n$  can be obtained by Eq. (10) and  $J_{n,D}$  can be obtained as below

Critical electric field for dynamic avalanche is expressed by Poisson equation using the current densities of  $J_{n,D}$  and  $J_{p,D}$  in the depletion layer.

$$E_{crit} = \frac{q}{\epsilon} \left( N_D + \frac{J_{p,D}}{qv_{sp}} - \frac{J_{n,D}}{qv_{sn}} \right) W(t) \quad (13)$$

where,  $E_{crit}$  is critical electric field,  $v_{sn}$  is electron saturation velocity in the depletion layer.

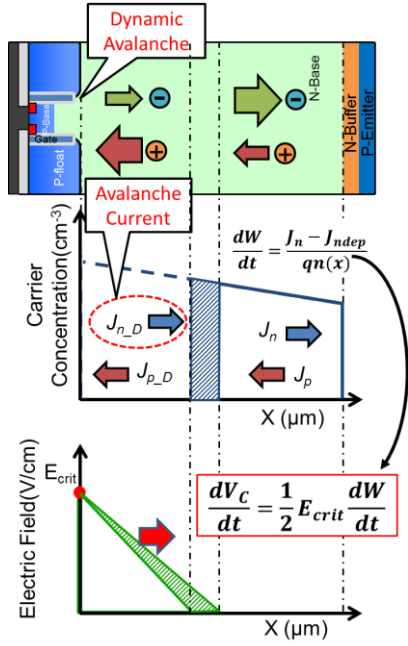


Fig. 5. Turn-off mechanism after dynamic avalanche the formulation.

In the depletion layer, hole current density  $J_{p\_D}$  is expressed by

$$J_{p\_D} = J_C - J_{n\_D} \quad (14)$$

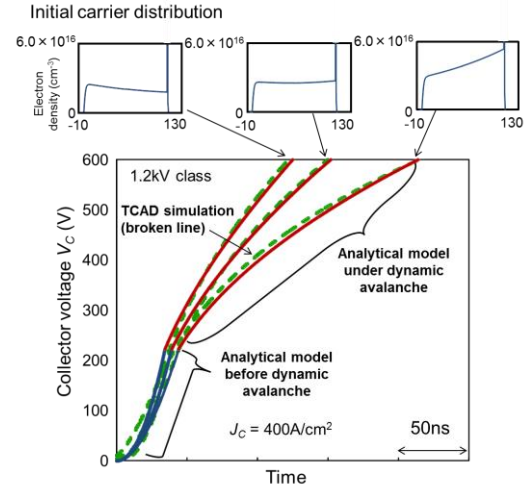
Substituting Eq. (14) into Eq. (13) and deforming the equation,  $J_{n\_D}$  can be obtained as

$$J_{n\_D} = \frac{v_{sp} v_{sn}}{v_{sp} + v_{sn}} \left( qN_D + \frac{J_C}{v_{sp}} - \frac{qE_{crit}}{W(t)} \right) \quad (15)$$

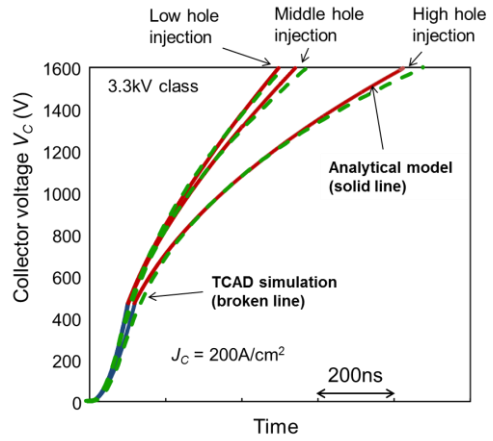
In this equation,  $W$  can be obtained by integration of Eq. (12).

### 2.3. Turn-off voltage waveform by new formulation combination

The turn-off model has been successfully verified by comparing with TCAD turn-off simulation for variety of initial carrier distribution in the N-Base and blocking voltage class (see Fig. 6). The analytical waveform is calculated by “Excel” (spreadsheet application) as linearly-approximated carrier distribution from TCAD simulation because we assume the lifetime is sufficiently long. Since the most of electric field during turn-off is sufficiently high to reach saturation velocity, we use constant saturation velocity for calculation (see Appendix). The conditions of the analytical calculation and the TCAD simulation are listed in the Table 1.

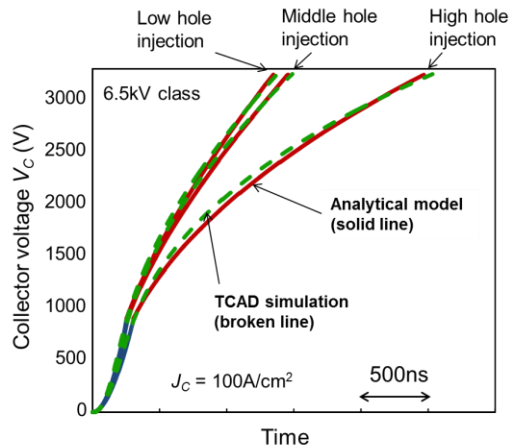


(a) 1.2 kV IGBT ( $k=1$ ,  $J_c=400A/cm^2$ ).



3.3 kV IGBT ( $k=1$ ,  $J_c=200A/cm^2$ ).

(b)



(c) 6.5kV IGBT ( $k=1$ ,  $J_c=100A/cm^2$ ).

Fig. 6. Turn-off waveform calculated by the proposed model formulation.

Table 1  
Parameters using analytical model and T-CAD simulation (k=1)

Parameters	
Half cell pitch	8.0 $\mu\text{m}$
Half mesa width	1.5 $\mu\text{m}$
Gate oxide thickness	0.1 $\mu\text{m}$
Electron mobility	1417 $\text{cm}^2/\text{Vs}$
Hole mobility	470.5 $\text{cm}^2/\text{Vs}$
Intrinsic carrier density	$1.18 \times 10^{10} \text{ cm}^{-3}$

The turn-off waveform is acquired by following circuit condition. Gate resistance and stray inductance are 0.1 $\Omega$  and 0.01 $\mu\text{H}$  respectively. DC voltage is around a half of blocking voltage. Current densities are 400A/cm<sup>2</sup> for 1.2 kV class, 200A/cm<sup>2</sup> for 3.3 kV class and 100A/cm<sup>2</sup> for 6.5 kV class.

### 3. Calculated trade-off curve with the proposed model

Trade-off curve between turn-off loss  $E_{off}$  and saturation collector voltage  $V_{Csat}$  calculated by the proposed model is sufficiently accurate as shown in Fig. 7 for the scaling factor of k=1 and 5 and blocking voltage class of 1.2 kV to 6.5 kV.

Saturation collector voltage  $V_{Csat}$  is calculated by analytical model for the on-state. A turn-off loss before reaching DC voltage and after reaching DC voltage is calculated separately. Before reaching DC voltage, current is assumed to be constant. So the loss is calculated by the integration of the product of constant collector current density  $J_C$  and collector voltage  $V_C$ . After reaching DC voltage, the loss is assumed to be product of remained stored charge in N-Base  $Q_{re}$  and DC voltage  $V_{DC}$ . The total turn-off loss is calculated by the sum of the losses.

### 4. Conclusion

Compact model for expressing turn-off waveform for advanced trench gate IGBTs is proposed under high current density condition. The model is analytically formulated only with device structure parameters. The validity of the model is confirmed with TCAD simulation. The proposed turn-off model is sufficiently accurate to calculate trade-off curve between turn-off loss and saturation collector voltage. The model can be used for system design with the

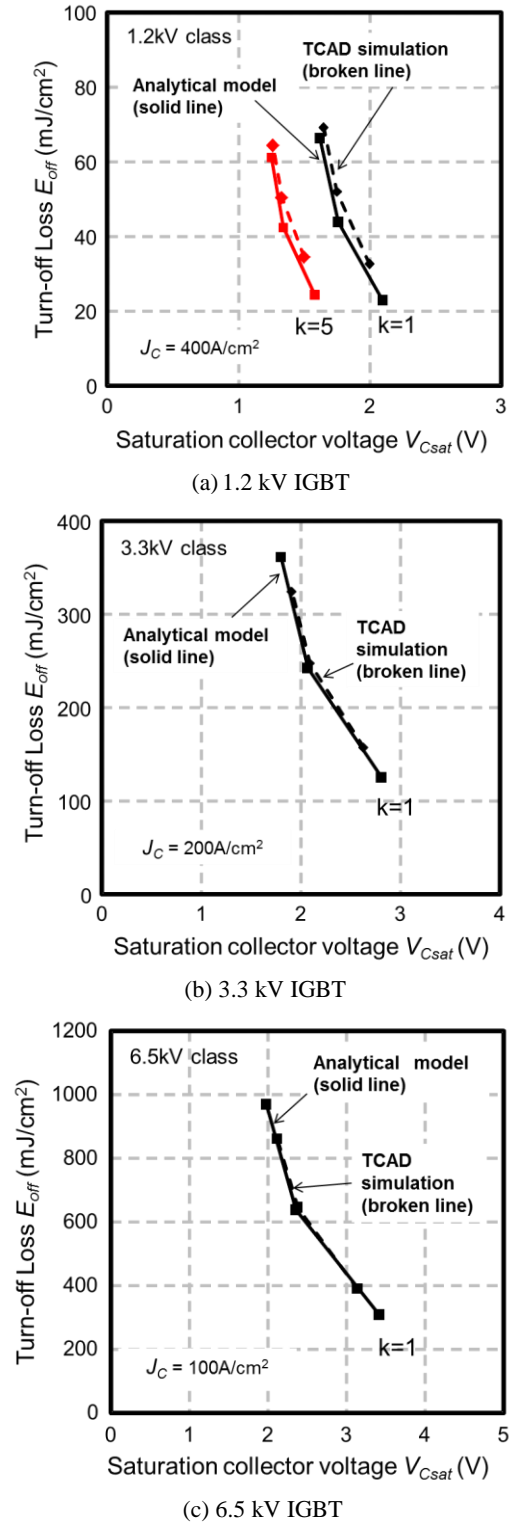


Fig. 7. Trade off curve obtained by the proposed model comparing to TCAD results.

advanced trench gate IGBTs.

## Acknowledgements

The authors would like to thank Masahiro Tanaka for useful discussion of the compact model for advanced trench IGBTs.

## Appendix

Electron and hole velocity with electric field during turn-off is shown in Fig. 8. The velocity is almost constant value around saturation velocity.

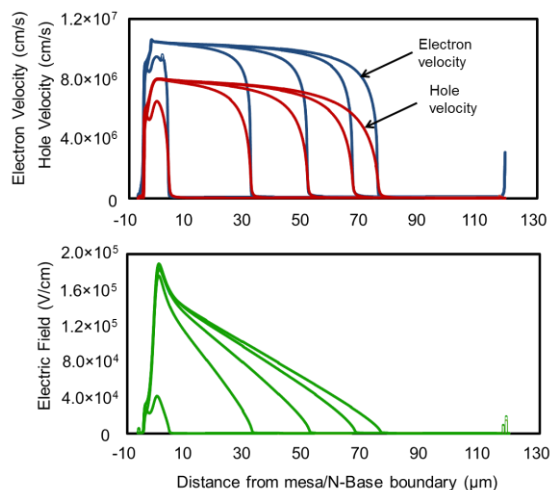


Fig. 8. Relation of electron and hole velocity with electric field during turn-off.

## References

[1] M. Tanaka, I. Omura, "Structure oriented compact model for advanced trench IGBTs without fitting parameters for extreme condition: Part I", Proc. Of 22<sup>nd</sup> European Symposium on the Reliability of Electron Devices, Failure Physics and Analysis, pp.1933-1937, 2011.

[2] M. Tanaka, I. Omura, "Scaling Rule for Very Shallow Trench IGBT toward CMOS Process Compatibility", Proc. Of 24<sup>th</sup> international Symposium on Power Semiconductor Devices & IC's(ISPSD), pp.177-180, 2012.

[3] M. Tanaka, I. Omura, "IGBT scaling principle toward CMOS compatible wafer processes" Solid-State Electronics, Vol. 80, pp.118-123, 2013.

[4] K. Seto, H. Imaki, J. Takaishi, M. Tanaka, M. Tsukuda. I. Omura, "Sub-micron Junction Termination for 1200V Class Devices toward CMOS Process Compatibility" Proc. Of 25<sup>th</sup> International Symposium on Power Semiconductor Devices & IC's(ISPSD), pp.281-284, 2013.

[5] R.H. Dennard, F.H. Gaensslen, V.L. Rideout, E. Bassous, A.R. LeBlanc, "Design Of Ion-implanted MOSFET's with Very Small Physical Dimensions", Solid-State Electronics, Vol. 9, Issue. 5, pp.256-268, 1974.

[6] Z. J. Shen, I. Omura, "Power Semiconductor Devices for Hybrid, Electric, and Fuel Cell Vehicles", Proc. Of IEEE, Vol. 95, Issue. 4, pp. 778-789, 2007.

[7] I. Omura, "Future role of power electronics", Proc. Of 6<sup>th</sup> International Conference on Integrated Power Electronics Systems (CHIPS), pp. 1-9, 2010.

[8] M. Kitagawa, I. Omura, S. Hasegawa, T. Inoue, A. Nakagawa, "A 4500V injection enhanced insulated gate bipolar transistor (IEGT) operating in a mode similar to a thyristor", IEDM Technical Digest, pp. 679-682, 1993.

[9] M. Harada, T. Minato, H. Takahashi, H. Nishihara, K. Inoue, I. Tanaka, "600V Trench IGBT in Comparison with Planar IGBT- An Evaluation of the Limit of IGBT Performance-", Proc. Of the 6<sup>th</sup> international Symposium on Power Semiconductor Devices & IC's(ISPSD), pp. 411-416, 1994.

[10] T. Laska, M. Munzer, F. Pfirsch, C. Schaeffer, T. Schmidt, "The Field Stop IGBT (FS-IGBT)—A new Power Device Concept with a Great Improvement Potential", Proc. Of 12<sup>th</sup> international Symposium on Power Semiconductor Devices & IC's(ISPSD), pp. 355-358, 2000.

[11] T. Matsudai, H. Nozaki, S. Umekawa, M. Tanaka, M. Kobayashi, H. Hattori, A. Nakagawa, "Advanced 60μm Thin 600V Punch- Through IGBT Concept for Extremely Low Forward Voltage and Low Turn-off Loss", Proc. Of 13<sup>th</sup> international Symposium on Power Semiconductor Devices & IC's(ISPSD), pp. 441-444, 2001.

[12] K. Hamada, T. Kushida, A. Kawahashi, M. Ishiko, "A 600V 200A low loss high current density trench IGBT for hybrid vehicle", Proc. Of 13<sup>th</sup> international Symposium on Power Semiconductor Devices & IC's(ISPSD), pp. 449-452, 2001.

[13] M. Baus, M.Z. Ali, O. Winkler, B. Spangenberg, Max C. Lemme, H. Kurz, "Monolithic Bidirectional Switch (MBS) – a novel MOS-based power device", Proc. Of 35<sup>th</sup> European solid-state device research conference (ESSDERC), pp.473-476, 2005.

[14] A. Nakagawa, "Theoretical Investigation of Silicon Limit Characteristics of IGBT", Proc. OF the 18<sup>th</sup> international Symposium on Power Semiconductor Devices & IC's(ISPSD), Session 1-2, 2006.

[15] M. Baus, B.N. Szafranek, S. Chmielus, M.C. Lemme, B. Hadam, B. Spangenberg, R. Sittig, H. Kurz, "Fabrication of Monolithic Bidirectional Switch (MBS) devices with MOS-controlled emitter structures", Proc. Of the 18<sup>th</sup> international Symposium on Power Semiconductor Devices & IC's(ISPSD), Session 6-28, 2006.

[16] M. Momose, K. Kumada, H. Wakimoto, Y. Onozawa, A. Nakamori, K. Sekigawa, M. Watanabe, T. Yamazaki, N. Fujishima, "A 600V Super Low Loss IGBT with Advanced Micro-P Structure for the next Generation IPM", Proc. Of the 22<sup>nd</sup> international Symposium on Power Semiconductor Devices & IC's(ISPSD), pp.379-382, 2010.

[17] M. Takaai, S. Fujikake, T. Naito, T. Kawashima, K. Shimoyama, H. Kuribayashi, "DB (Dielectric Barrier) IGBT with extreme injection enhancement", Proc. Of the 22<sup>nd</sup> international Symposium on Power Semiconductor Devices & IC's(ISPSD), pp. 383-386, 2010.

[18] M. Tsukuda, I. Omura, Y. Sakiyama, M. Yamaguchi, K. Matsushita, T. Ogura, "Critical IGBT Design Regarding EMI and Switching Losses" Proc. Of 20<sup>th</sup> International Symposium on Power Semiconductor Devices & IC's(ISPSD), pp.185-188, 2008.